

On-line Digital Holographic Measurement of Size and Shape of Microparticles for Crystallization Processes

Taslina Khanam,^a Emmanouil Darakis,^{c,a} Arvind Rajendran,^a Vinay Kariwala,^a
Anand K. Asundi,^b and Thomas J. Naughton,^{c,d}

^aSchool of Chemical and Biomedical Engineering, Nanyang Technological University,
Singapore, 637459;

^bSchool of Mechanical and Aerospace Engineering, Nanyang Technological University,
Singapore, 639798;

^cDepartment of Computer Science, National University of Ireland, Maynooth,
County Kildare, Ireland;

^dUniversity of Oulu, RFMedia Laboratory, Oulu Southern Institute, Vierimaantie 5,
84100 Ylivieska, Finland

ABSTRACT

Crystallization is a widely used chemical process that finds applications in pharmaceutical industries. In an industrial crystallization process, it is not only important to produce pure crystals but also to control the shape and size of the crystals, as they affect the efficiency of downstream processes and the dissolution property of the drug. The effectiveness of control algorithms depend on the availability of on-line, real-time information about these critical properties. In this paper, we investigate the use of lens-less in-line digital holographic microscopy for size and shape measurements for crystallization processes. For this purpose, we use non-crystalline spherical microparticles and carbon fibers with known sizes present in a liquid suspension as test systems. We propose an algorithm to extract size and shape information for a population of microparticles from the experimentally recorded digital holograms. The measurements obtained from the proposed method show good agreement with the corresponding known size and shape of the particles.

Keywords: Crystallization; Digital holography; On-line measurement; Particle size distribution.

1. INTRODUCTION

Crystallization is an important solid-liquid separation process that results in solid crystals from an impure solution. Crystals formed in this way are nearly pure and this aspect enables its application in various sectors of chemical process industries, especially in fine chemical and pharmaceutical industries. Post processing of the crystals is usually performed by a series of steps such as filtration, washing and drying to separate the crystals from the slurry.^{1,2} The effectiveness of these steps depends on crystal size and shape obtained during crystallization step. Furthermore, crystal shape is another important factor whose effect is mainly observed in the crystallization of pharmaceutical products. Both crystal size and shape significantly affect the dissolution properties of drug.³ For these reasons, it is important to control crystallization processes in order to obtain a desirable crystal shape and size distribution.

The commonly used methodology to optimize the performance of crystallizers and the downstream process, is to implement feedback control schemes. A schematic of a feedback control system for a crystallization process is shown in Fig. 1. The system has three elements: the crystallizer, monitoring tools and the controller. The on-line monitoring tools are used to measure key process parameters. The 'measured' variables are compared to desired 'set-points' by the controller which then decides upon the control action by suitably adjusting the 'manipulated variables'. In crystallization processes, the measured variables are the temperature, concentration of solids, crystal size distribution (CSD) and crystal

Further author information: T. Khanam: tasl0001@ntu.edu.sg, E. Darakis: emmdarakis@ieee.org, A. Rajendran: arvind@ntu.edu.sg, V. Kariwala: vinay@ntu.edu.sg, A. K. Asundi: anand.asundi@gmail.com, T. J. Naughton: tomn@cs.nuim.ie

Ninth International Symposium on Laser Metrology, edited by Chenggen Quan, Anand Asundi
Proc. of SPIE Vol. 7155, 71551K, (2008) · 0277-786X/08/\$18 · doi: 10.1117/12.814557

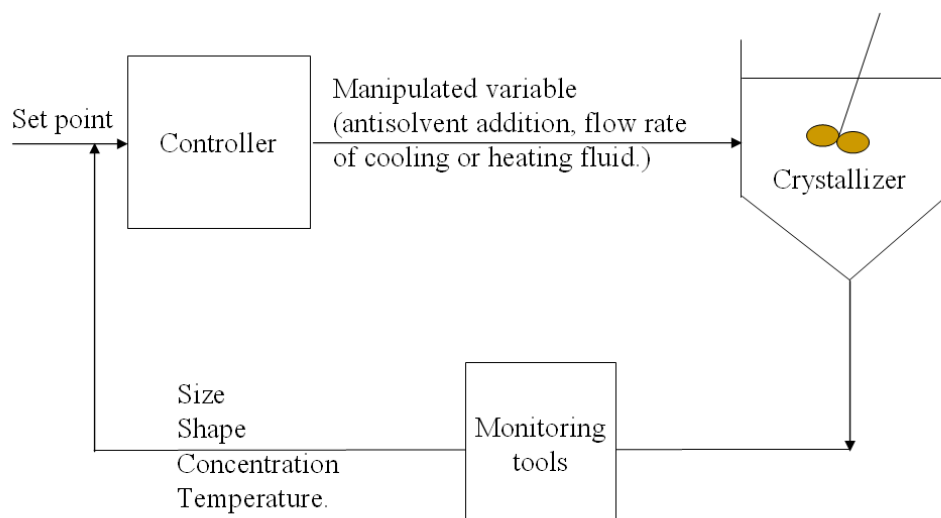


Fig. 1. Feedback control of a crystallizer

shape while the manipulated variables are typically flow rate of cooling medium, rate of anti-solvent addition etc.² The performance of the controller action directly depends on the reliability of the on-line measurement tool. Hence there is a clear need for the development of reliable monitoring tools.

Currently several techniques are used as monitoring tools for crystallization process.² The Lasentec focused beam reflectance measurement (FBRM) is the most commonly used in-situ technique for measuring size distribution.⁴⁻⁶ It uses a highly focused laser beam rotating with a high speed that rapidly scans over a small region of particles suspensions. When particles come in the field of the rotating beam, they result in backscattered light which is recorded by a detector. Backscattering continues until the rotating beam completes scanning from one edge to another edge of particle. The timespan of scanning is multiplied by the scan speed of the rotating beam to give the distance between two edges of the particle, i.e. chord length. Though this technique can be used to measure crystals in the size range of microns, it has an important shortcoming as the measured chord length distribution (CLD) has to be converted to particle size distribution (PSD) in order to be used for control purposes. This conversion, however relies on the assumptions about the particle shape.^{5,7} The use of video microscopy is another established technique in the field of particle size and shape measurement.^{8,9} This imaging based technique, which nevertheless simplifies the experimental set-up and reduces the cost, has certain limitations as well. These limitations mainly arise from limited depth of focus imposed by the required magnification. This results in the captured images containing blurred and out-of-focus objects that limits the successful application of image analysis for acquiring particle sizes and shapes.⁸⁻¹⁰ Hence, there is strong need to develop appropriate on-line sensors for the monitoring of crystallization process, which might overcome the prevailing shortcomings.

Holography is a popular method in the field of imaging due to its capability of restoring three dimensional volume information from a single hologram acquisition. Thus, holography, compared to other imaging techniques, neither encounters the problem of out-of-focus objects, nor does require conversion of measured quantity to size and shape information. In comparison with classical film based holography, use of digital holography is more attractive due to the ease of set-up and recording process.^{11, 12} In this work, we benchmark digital holographic microscopy as a monitoring tool for the measurement of crystal size and shape. For this purpose we use non-crystalline microparticles suspended in water that are representative of particles encountered in real crystallizers, as test systems. In particular, we will investigate two classes of particles, namely, spherical and fibers. These represent the extremes of particles encountered in crystallization, i.e. spheres and needles and hence prove to be ideal for benchmarking. We also propose an algorithm which automatically quantifies the particle size distribution (PSD) and shape from an experimentally recorded hologram. This proposed technique, when combined with appropriate control algorithms, can enable the satisfactory control of crystallization processes.

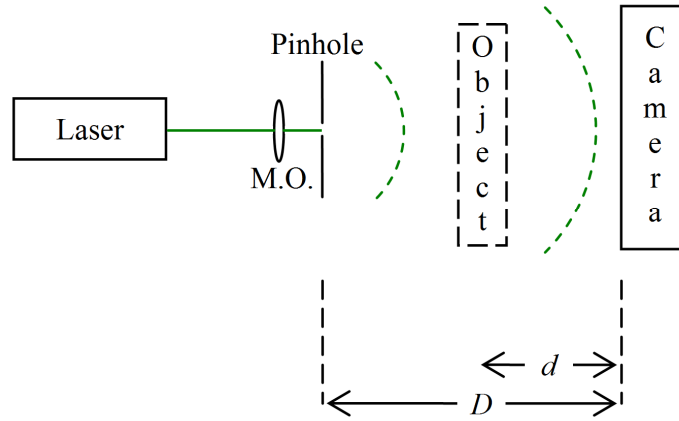


Fig. 2. Digital holographic microscopy setup. M. O. stands for Microscopic Objective lens.

The paper is organized as follows: In Section 2, fundamentals of in-line digital holography along with the recording set-up and a brief outline of the proposed algorithm that is used for processing of holograms and extraction of particle size are described. Section 3 describes the experimental procedure along with results in details. Finally we conclude Section 4.

2. IN-LINE DIGITAL HOLOGRAPHIC MICROSCOPY

2.1 Digital holography recording and reconstruction

The setup for the recording of the digital holograms is shown in Fig. 2. A laser beam is focused by a microscopic objective lens onto a pinhole which is located at a distance D from the recording camera. The resulting spherical diverging beam originating from the pinhole illuminates the object, a diffusely reflecting body which is located at a distance d from the recording camera. One part of the illuminating beam passes through the object without being diffracted and acts as the reference beam U_R . Another part of the illuminating beam is diffracted by the particles within the sample, generating the object beam U_d which propagates towards the recording camera. The interference pattern between the reference and the object waves results in hologram. The spherical diverging reference beam U_R can be expressed as¹¹

$$U_R(x, y) = \frac{\exp\left(-i \frac{2\pi}{\lambda} \sqrt{x^2 + y^2 + D^2}\right)}{\sqrt{x^2 + y^2 + D^2}}, \quad (1)$$

where x and y are the spatial coordinates on the camera plane, and λ is the wavelength of the laser beam. The object beam U_d at the camera plane can be expressed by the Fresnel-Kirchhoff integral as¹¹

$$U(x, y) = \int_{-\infty}^{+\infty} \int_{-\infty}^{+\infty} U_d(x', y') \frac{\exp\left[-i \frac{2\pi}{\lambda} \sqrt{(x'-x)^2 + (y'-y)^2 + d^2}\right]}{\sqrt{(x'-x)^2 + (y'-y)^2 + d^2}} dx' dy', \quad (2)$$

where x' , y' are the spatial coordinates on the object plane. For simplicity, constant phase terms have been neglected in Eq. 2.

The resulting hologram captured by a CCD camera can be expressed as

$$I(x, y) = [U_R(x, y) + U(x, y)]^2. \quad (3)$$

For the reconstruction of the hologram at a distance d' , I has to be multiplied by the reference wave and then propagated using the Fresnel-Kirchhoff integral as¹¹

$$U_{d'}(x', y') = \int_{-\infty}^{+\infty} \int_{-\infty}^{+\infty} I(x, y) U_R(x, y) \frac{\exp\left[-i \frac{2\pi}{\lambda} \sqrt{(x-x')^2 + (y-y')^2 + d'^2}\right]}{\sqrt{(x-x')^2 + (y-y')^2 + d'^2}} dx dy. \quad (4)$$

In digital holographic microscopy, Eq. 4 has to be numerically calculated with the convolution method.¹¹ For $d'=d$ and when quantization and other digitizing errors are negligible, the reconstructed wave $U_{d'}$ equals to the object wave U_d . For the reconstruction process, convolution method is used in where the pixel size of the reconstructed image ($\Delta x'$, $\Delta y'$) equals the pixel size of the recording camera (Δx , Δy), i.e. $\Delta x' = \Delta x$ and $\Delta y' = \Delta y$.¹¹ The diverging beam used in the system offers magnification allowing the study of smaller particles. Hence, lateral magnification, defined as $M(d) = r'(d)/r$, where $r'(d)$ is the measured size of the object at distance d and r is the real object size, can be introduced by changing the distance between the point source of the spherical reference wave and the CCD, or the wavelength that is used for the reconstruction as¹¹

$$M(d) = \left(1 + \frac{d}{D'} \frac{\lambda}{\lambda'} - \frac{d}{D}\right)^{-1}, \quad (5)$$

where D' is the pinhole to CCD distance and λ' is the wavelength which is used for the reconstruction. By changing D' and λ' , the distance d' , where the object will appear focused, also changes as¹¹

$$d' = \left(\frac{1}{D'} + \frac{\lambda'}{\lambda} \frac{1}{d} - \frac{1}{D} \frac{\lambda'}{\lambda}\right)^{-1}. \quad (6)$$

For our experiments, we change only D' as $D' = 100 D$ and retain $\lambda' = \lambda$.

2.2 Extraction of particle size

There are algorithms available for the extraction of particle properties, such as the size and the depth, from hologram without reconstruction.¹³⁻¹⁵ Nevertheless these algorithms assume spherical particles and hence cannot be used for monitoring of crystal size and shape.

The measuring algorithm that has been used is described in more details elsewhere.¹⁶ For the sake of completeness it is briefly described here. The hologram is reconstructed at several depths covering the volume to be examined. Canny edge detection¹⁷ is used to identify particles on each reconstruction. The intensity of each identified area is compared to the mean intensity of the reconstruction and only dark areas are considered. This is done in order to avoid considering areas of the background which might happen to be surrounded by strong edges. Also areas touching the edges of the reconstruction are neglected to avoid erroneous size measurements.

For each reconstruction and for each identified particle several properties, such as its spatial location, its area in pixels, and a focusing metric, are recorded. This results in a list of all the identified particles. Each particle might appear several times in the list at different depths, but always at the same x-y location. Hence the multiple occurrences of each particle can be grouped together based on their location on the reconstruction. Each such group corresponds to a single particle, and the focusing metric is used to select the best focusing depth of the particle. The area of the particle at this depth is also selected as the best estimate of the particle's area. This procedure results in a list of uniquely identified and focused particles containing information such as their spatial location, depth and area.

In order to measure the size of the area, some assumptions have to be made. For example, assuming circular particles, the equivalent diameter of the area can be calculated as the diameter of a circle with same area as the particle. In case of ellipsoid particles, an ellipse with the same normalized second central moments as the identified region can be used to calculate the lengths of the major and the minor axes.

Table 1. Characteristics of various particles used in the study

<i>Experimental system</i>	<i>Average mean size</i>	<i>Shape</i>	<i>Transparency</i>	<i>Specific gravity</i>
Ceramic beads on glass slide	Diameter $\approx 80 \mu\text{m}$	Spherical to elliptical	Opaque	High
Carbon fibers in suspensions	Diameter $\approx 9 \mu\text{m}$, length $\approx 50 - 500 \mu\text{m}$	Needle	Opaque	Low
Polymer particles in flow system	Diameter = $40 \mu\text{m}$	Spherical	Opaque	Medium

In order to convert the measured size (i.e. in pixels) to the real length, the value needs to be converted using the magnification factor M as

$$r = \frac{r_{\text{pixels}} \Delta x}{M(d_o)}, \quad (7)$$

where r_{pixels} is the measured size of the particle in pixels, Δx is the pixel size of the recording camera, and $M(d_o)$ is the magnifying factor at the best focusing depth of each particle.

3. EXPERIMENTS AND RESULTS

Several experiments were conducted in approaching to the goal of digital holography based particle analysis in the monitoring of crystallization process using the digital holographic recording set-up shown in Fig. 2. Each experimental system along with particle characteristics are summarized in Table 1. Three categories of experiments were performed. The first set of experiments dealt with ceramic beads (diameter $\approx 80 \mu\text{m}$) placed on glass slide. The second set consisted of imaging carbon fibers (diameter $\approx 9 \mu\text{m}$) in suspension. Finally, the last set consisted of imaging polymer particles in suspension using a flow through system. The recording set-up was used with a green laser of wave length 532 nm, a 60 \times microscopic objective lens and 1 μm pinhole. The distance between the point source and the CCD camera for the recording was $D \approx 62 \text{ mm}$ and for the reconstruction a point source to CCD camera distance of $D' = 100 D = 6.2 \text{ m}$ was used. The camera used for the experiments had 1280 \times 960 square pixels of size $\Delta x = \Delta y = 4.65 \mu\text{m}$. The obtained resolution tested by USAF target for $D \approx 62 \text{ mm}$ was $\approx 7 \mu\text{m}$.

3.1 Microspheres on glass slide

In order to assess the proposed digital holography microscopy for the monitoring of crystal size and shape, non-crystalline ceramic beads with average particle size of $\approx 80 \mu\text{m}$ were used. This experiment consisted of imaging a population of ceramic beads placed on glass slide. The slide was positioned normal to the optical axis so that the diverging beam of the light illuminates an area of glass slide containing a population of ceramic beads. A hologram for this system was recorded. A series of experiments were carried out in a similar fashion to account for a population of particles. The recorded holograms were processed following the procedure described in Section 2.2, whose details can be found elsewhere.¹⁶ For the reconstruction of each hologram, a step size of 50 μm covering a volume of depth size of 3 mm was used.

Fig. 3 (a) shows one of the recorded holograms of ceramic beads and the corresponding reconstructed image is shown in Fig. 3 (b). The algorithm described in Section 2.2 identified approximately 440 different particles from several holograms. Care was taken not to obtain duplicate images of the same area. The resulting PSD measurements and axis length distribution (ALD) from the holograms is shown in Fig. 4 (a) and Fig. 4 (b). The mean particle size identified from the holographic microscopy was 81.1 μm and the standard deviation was 14.61 μm , which showed a good agreement with the particle size distribution which was measured using a scanning electron microscopy (SEM).¹⁶ Fig. 4 (b) shows the ALD of ceramic beads. It can be seen that the major to minor axis length ratio, or aspect ratio for most of particles close to 1 which ultimately provides the information about the sphericity of the particles. As can be seen, there

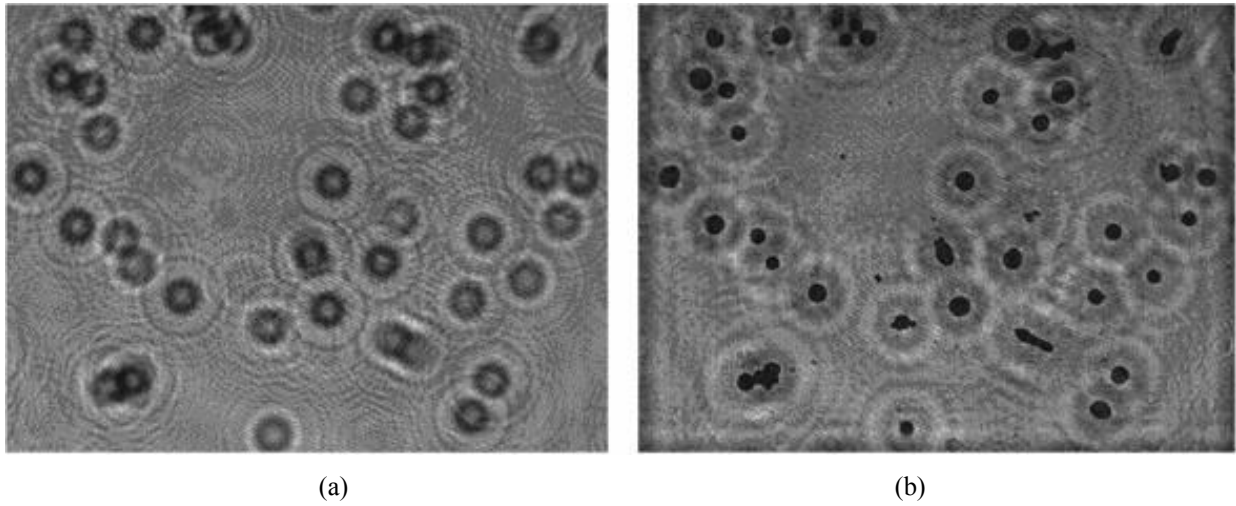


Fig. 3. Digital holographic microscopy data of ceramic beads on glass slide. (a) One of the recorded digital holograms and (b) Example of a reconstructed image

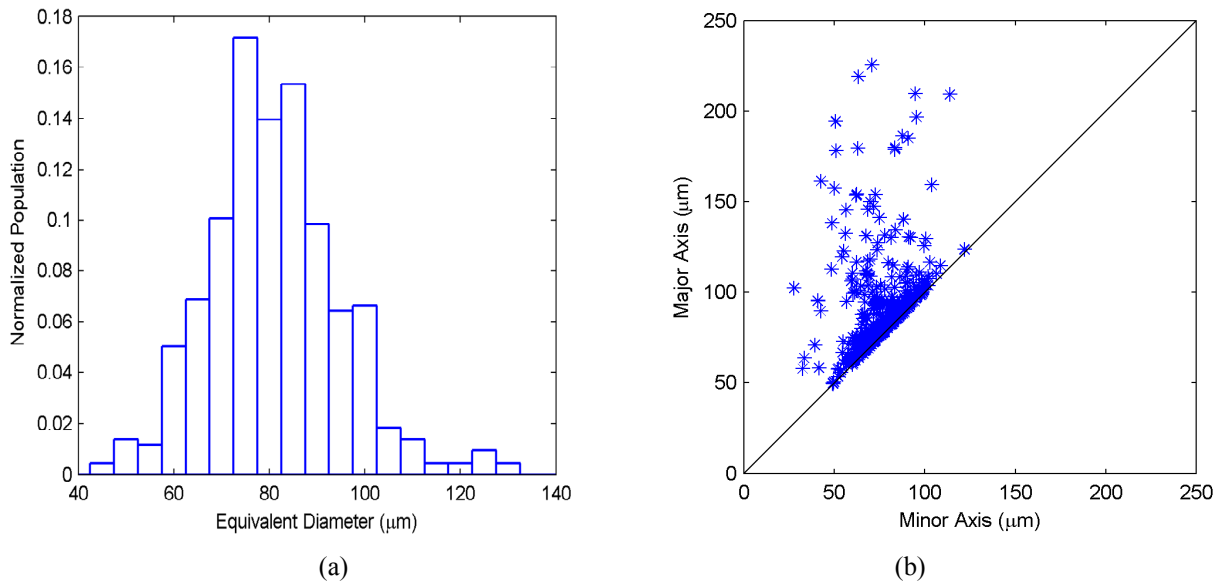


Fig. 4. (a) Particle size distribution of ceramic beads obtained by digital holographic microscopy method. (b) Axis length distribution of spherical ceramic beads. Each asterisk represents the axis length of one particle.

were particles that were not perfectly symmetrical, hence leading to aspect ratios greater than 1. Visual inspection of particles from reconstructed hologram shown in Fig. 3 (b) clearly indicates these particles.

3.2 Carbon fibers suspended in water

In this experiment, we studied carbon fibers with diameter of $\approx 9 \mu\text{m}$ and with length in the range 50-500 μm suspended in water. The sample contained in a 12.5 mm (L) \times 12.5 mm (W) \times 48 mm (H) glass cuvette was examined. The optical path length of the cuvette was 10mm and one hologram was recorded for the system. The hologram was reconstructed with a step size of 25 μm between each other so that an overall depth of 10 mm (equal to the optical path length) was covered.

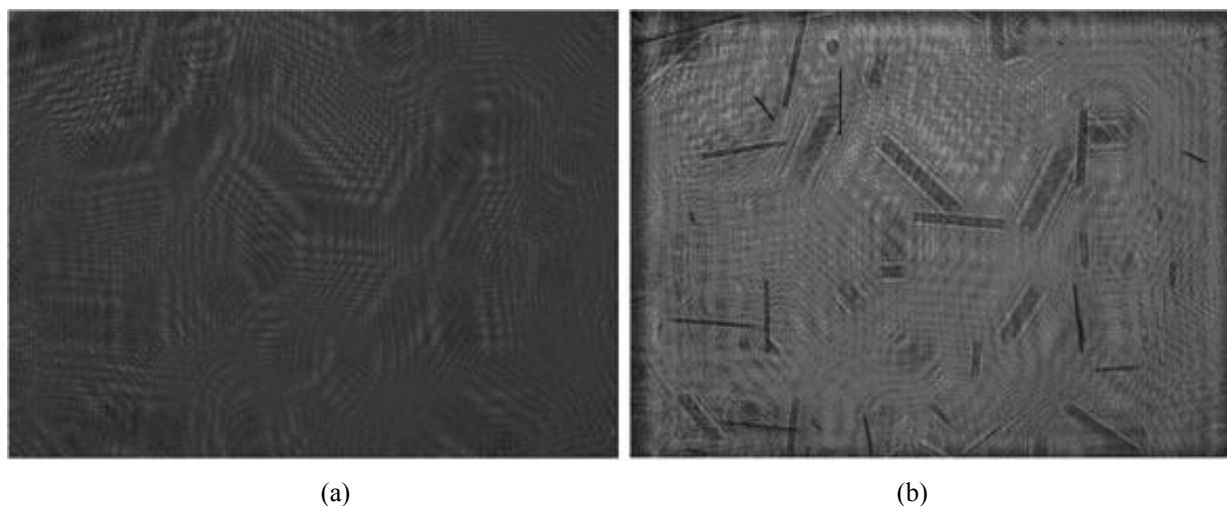


Fig. 5. Digital holographic microscopy data of carbon fiber suspended in water. (a) A recorded digital hologram and (b) Example of a reconstructed image.

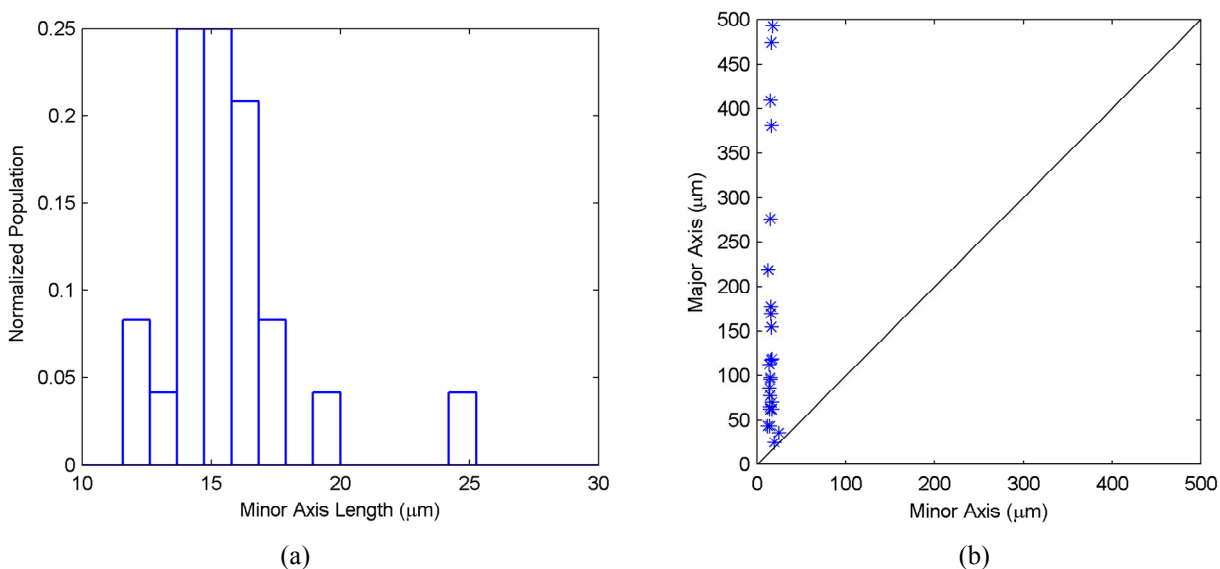


Fig. 6. (a) Minor axis length distribution of carbon fiber and (b) Axis length distribution of carbon fibers.

A hologram and a reconstructed image of carbon fiber suspension is shown in Fig. 5 (a) and Fig. 5 (b), respectively. Twenty four different fibers were identified from the hologram. The resulting minor axis length distribution and ALD are shown in Fig. 6 (a) and Fig. 6 (b), respectively. The obtained mean diameter of carbon fiber was $15.62 \mu\text{m}$ and the standard deviation was $2.49 \mu\text{m}$. The diameter of the fiber is very close to the resolution limit of the system that results in relatively large spread around the expected size which can be observed in Fig. 6 (a). In Fig. 6 (b), it is observed that the resulting ALD is almost a vertical line at $x \approx 15$ attributing to needle like shape of particles.

3.3 Flow-through-system

For this experiment, the object used in the set-up consisted of a flow cell with flowing particle suspensions. The National Institute of Standards and Technology (NIST) certified polymer microspheres manufactured by Duke Scientific Corporation, USA with diameter of $40 \mu\text{m}$ were continuously pumped from a beaker through circulation loop using a peristaltic pump. The particles flowed through a flow cell equipped with quartz windows which enabled the imaging.

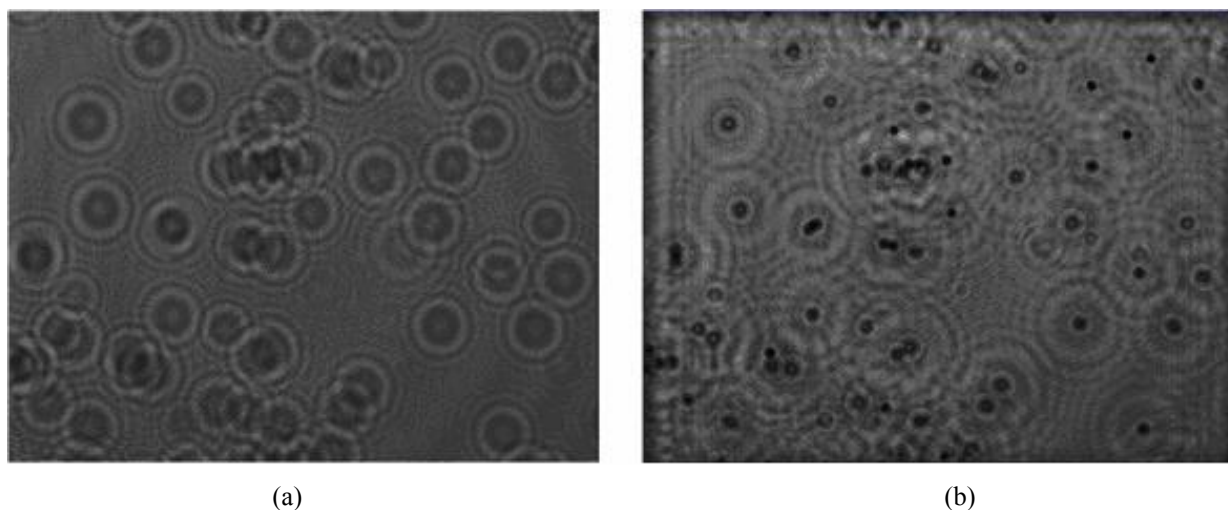


Fig. 7. Digital holographic microscopy data of 40 μm polymer microsphere suspensions through flow cell. (a) A recorded digital hologram and (b) Example of a reconstructed image.

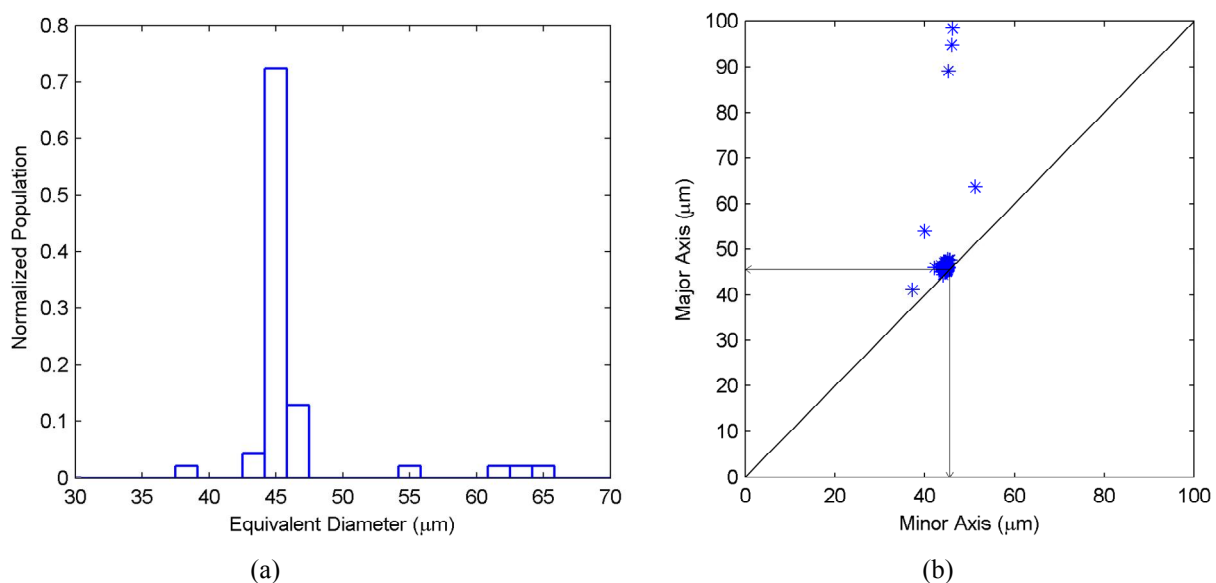


Fig. 8. (a) Particle size distribution of 40 μm polymer microspheres and (b) Axis length distribution of 40 μm polymer microspheres

Holograms of the flowing particle suspensions through a 12.5 mm (L) \times 12.5 mm (W) \times 65 mm (H) flow cell with a optical path length of 10 mm were captured (one hologram per second) by the CCD. Reconstructions were carried out with a distance of 25 μm between each other covering a volume of depth size of 8 mm. The purpose of using this flow cell system is to closely match the conditions that will be encountered during the application of the developed technique to crystallization processes.

Fig. 7 (a) shows one of the recorded holograms of 40 μm polymer particles suspensions in flow cell and the corresponding reconstructed image is shown in Fig. 7 (b). The algorithm identified 47 different particles. The resulting PSD and ALD are shown in Fig. 8 (a) and Fig. 8 (b) respectively. The obtained mean particle size was 46.49 μm and the standard deviation was 4.97 μm . There is an error of ≈ 6 μm between the actual particle size and the location of the PSD peak. This error is below the resolution of the system (the obtained resolution for $D \approx 62$ mm was ≈ 7 μm). The error can partially be attributed to inaccurate measurement of the distance D between the point source and the recording camera, which for practical reasons, cannot be measured accurately. In Fig. 8 (a), a spread in PSD around the diameter 60-65 μm

is also observed. This indicates the presence of agglomerated particles. In Fig. 8 (b), the obtained ALD confirms the spherical shape of particles, as a majority of the particles are found to have identical major and minor axes.

4. CONCLUSIONS

This paper has shown that digital holography can successfully measure the particle size and shape using a simple user-defined algorithm. A series of experiments were described to investigate the use of digital holography for dried, suspended and flowing systems of microparticles. The resulting measurements showed similar performance of the developed algorithm for each system. The flow cell system can be used for on-line monitoring of crystal size and shape. For the carbon fiber suspensions and polymer microsphere flow cell system, the algorithm scanned a volume of depth ≈ 10 mm and successfully performed automatic focusing and quantification of particle size and shape. Hence it overcomes the challenge concerning out-of-focus objects within a volume of depth encountered in the field of photography. Two different shapes of particles: carbon fibers (needle shape) and microspheres were studied and the results clearly revealed the information of the respective shape of those particles without prior knowledge of aspect ratio. All results about the size and shape measurements based on digital holography microscopy obtained in this paper show good agreement with the given sizes and shapes measured by independent techniques. Though results obtained using digital holography microscopy measurement were satisfactory, several issues such as presence of high density crystals, transparent or semi transparent particles, dynamic growth of crystals in the crystallization process need to be addressed prior to the satisfactory implementation of digital holography based particle size and shape measurement system for the monitoring of crystallization process.

ACKNOWLEDGMENTS

This work is partially supported by the Office of Research, Nanyang Technological University through grant no. RG25/07 and partially by the Irish Research Council for Science, Engineering and Technology under the National Development Plan through grant no. PD/2007/11. The authors would like to thank Vijay Raj Singh and Qu Weijuan for assisting with the recording setup.

REFERENCES

- [1] Mullin, J. W., [Crystallization], Butterworth-Heinemann, Oxford (2001).
- [2] Larsen, P. A., Patience, D. B., and Rawlings, J. B., "Industrial crystallization process control", *Contr. Syst. Mag.* 26(4), 70-80 (2006).
- [3] Winn, D. and Doherty, M. F., "Modeling crystal shapes of organic materials grown from solution," *AIChE J.* 46(7), 1348-1363 (2000).
- [4] Abbas, A., Nobbs, D., and Romagnoli, J. A., "Investigation of on-line optical particle characterization in reaction and cooling crystallization systems: Current state of the art," *Meas. Sci. Technol.* 13(3), 349-356 (2002).
- [5] Ruf, A., Worlitschek, J., and Mazzotti, M., "Modeling and experimental analysis of PSD measurements through FBRM," *Part. Part. Syst. Char.* 17(4), 167-179 (2000).
- [6] Kougoulos, E., Jones, A. G., Jennings, K. H., and Wood-Kaczmar, M. W., "Use of focused beam reflectance measurement (FBRM) and process video imaging (PVI) in a modified mixed suspension mixed product removal (MSMPR) cooling crystallizer," *J. Cryst. Growth* 273(3-4), 529-534 (2005).
- [7] Li, M., Wilkinson, D., and Patchigolla, K., "Obtaining particle size distribution from chord length measurements," *Part. Part. Syst. Char.* 23(2), 170-174 (2006).
- [8] Patience, D. B. and Rawlings, J. B., "Particle-shape monitoring and control in crystallization processes," *AIChE J.* 47(9), 2125-2130 (2001).
- [9] Larsen, P. A., Rawlings, J. B., and Ferrier, N. J., "Model-based object recognition to measure crystal size and shape distributions from in situ video images," *Chem. Eng. Sci.* 62(5), 1430-1441 (2007).
- [10] Calderon De Anda, J., Wang, X. Z., Lai, X., and Roberts, K. J., "Classifying organic crystals via in-process image analysis and the use of monitoring charts to follow polymorphic and morphological changes," *J. Process Contr.* 15(7), 785-797 (2005).
- [11] Schnars, U. and Juptner, W., [Digital Holography: Digital Hologram Recording, Numerical Reconstruction, and Related Techniques], Springer, Berlin (2005).
- [12] Xu, W., Jericho, M. H., Meinertzhagen, I. A., and Kreuzer, H. J., "Digital in-line holography of microspheres," *Appl. Opt.* 41(25), 5367-5375 (2002).

- [13] Buraga-Lefebvre, C., Coetmellec, S., Lebrun, D., and Ozkul, C., "Application of wavelet transform to hologram analysis: Three-dimensional location of particles," *Optics Las. Eng.* 33(6), 409-421 (2000).
- [14] Denis, L., Fournier, C., Fournel, T., Ducottet, C., and Jeulin, D., "Direct extraction of the mean particle size from a digital hologram," *Appl. Opt.* 45(5), 944-952 (2006).
- [15] Soontaranon, S., J., W., and Asakura, T., "Extraction of object position from in-line holograms by using single wavelet coefficient," *Optics Commun.* 281(6), 1461-1467 (2008).
- [16] Darakis, E., Khanam, T., Rajendran, A., Kariwala, V., Naughton, T. J., and Asundi, A. K., "Processing of digital holograms for size measurements of microparticles," in *Proceedings of the 9th International Symposium on Laser Metrology*, Asundi, A. K., ed., In Press, SPIE (2008).
- [17] Canny, J., "Computational approach to edge detection," *IEEE T. Pattern Anal.* 8(6), 679-698 (1986).